Allosteric inhibition of VIMs metallo-β-lactamases by a camelid single-domain antibody fragment.

Sohier JS[1], Laurent C[1], Chevigné A[3], Pardon E[2], Srinivasan V[2], Lassaux P[1], Buys N[2], Willibal K[2], Steyaert J[2] and Galleni M[1]

[1]Centre for Protein Engineering, Macromolécules Biologiques lab, University of Liege, Belgium
[2] Department of Molecular and Cellular Interactions (VIB), Structural Biology Brussels lab, Free University of Brussels, Belgium
[3] Virology, Allergology and Immunity Deparment, Laboratory of Retrovirology, Centre de Recherches Public (CRP-Santé), Luxembourg

Metallo-β-lactamases (MβLs) are zinc dependant enzymes able to hydrolyze a broad spectrum of clinically useful β-lactam antibiotics, including the most powerful carbapenems. These enzymes are not susceptible to classical β-lactamase inhibitor so that their worldwide spread, especially amongst multiresistant Gram-negative strains, makes urgent a better understanding of these enzymes in order to discover new drugs. The selection of broad spectrum inhibitors against metallo-β-lactamases is made difficult first, by the diversity among MβLs which are classified in 3 subclasses, secondly by their mechanism which does not include any highly populated metastable reaction intermediates and finally by the fact that the compound must remain inactive towards similar human proteins.

In this context, we have selected from two immune libraries of phages, 55 heavy chain antibody fragments (V_HH) able to bind the clinically relevant MβL VIM-4. A phage display experiment that was performed in solution by using biotinylated VIM-4 allowed us to select one inhibiting dromedary V_HH termed CA1838. This inhibiting V_HH was fused to the "cherry" protein in order to overproduce it in *E.coli*. The inhibition is in the µM range for all the β-lactams assayed and, with cephalotin, has been found to be mixed hyperbolic with a predominant uncompetitive component. Moreover, a substrate inhibition occurred only when the V_HH is bound.

With the aim of identifying binding hot-spots of CA1838, VIM-4 residual activities were measured in presence of 17 alanine mutants of the V_HH. The main binding determinant of the paratope is a stretch of 6 hydrophobic amino acids in the CDR3. (T107, Y108, V109, F110, F112.2 and L114) Peptide-arrays allowed us to identify a conformational epitope on VIM-4 which corresponds mainly to the hydrophobic loop L6 and the C-terminal end of the helix α2. As this binding site is distant from the active-site and alters both substrate binding and catalytic properties of VIM-4, this V_HH qualify to the definition of an allosteric effector. Therefore, the binding of cherry-CA1838 could inhibit the enzyme by interfering with molecular motion required for efficient catalysis. We hypothesized that the amino-acids stretch whose dynamic would be affected could correspond to the N-terminal part of helix α2 which is in direct connection with the active site loop L7.

Thus, this work is another indication of the dynamic nature of metallo-β-lactamases, and the different V_HHs that have been selected could be useful for the resistance typing of pathogenic strains.

I. Phage Display

A selection of V_HHs that was performed in solution allows the identification of CA1838 as an inhibitor of VIM-4.

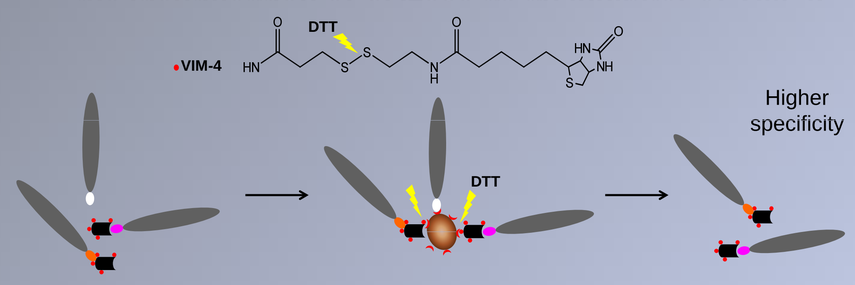

In order to increase the specificity and the diversity of the V_HHs, the selection was realised in solution using magnetic beads and Sulfo-NHS-SS-Biotin (Pierce). 55 different V_HHs could be obtained among which the only inhibitor CA1838. This V_HH was fused to the so-called cherry protein in order to over produce it in *E.coli*.

II. Paratope analysis

The main part of the interaction is driven by the hydrophobic stretch $T_{107}YVF_{110}$ which is in the N-terminal part of the CDR3 loop. These residues are probably present at the interface between the two proteins.

A.

```
    5         15         25         35
....|....|....|....|....|. ...|....|...
QVQLQESGG-GSVQAGGSLRLSCAAS GYSI----SSGC
<--------FR1--IMGT-------> <CDR1--IMGT>

      45         55         65
.|....|....|....| ....|....|
MGWFRQAPGKQREGVAS ISRD--GNTA
<---FR2--IMGT---> <CDR2IMGT>

         75         85         95
....|....|....|....|....|....|....|....
VYADSVK-GRFTISQDNAKNTVYLLMNSLKPEDTAIYYC
<--------------FR3--IMGT-------------->

105    1234554321         120
|....|....|....|....|.. ..|....|...
AATYVFPCTN---PGFSEYLYNY WGQGTQVTVSS
<-----CDR3--IMGT------> <FR4—IMGT>
```

B.

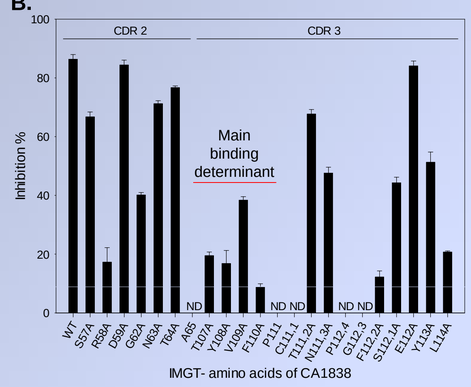

A. Primary structure of the V_HH CA1838. V_HH's hallmarks amino-acids are in bold. Residues subjected to alanine scanning are in red. (IMGT numbering)
B. Alanine-scan of CA1838's paratope. ND: not determined

III. Steady state kinetics

The inhibition is in the µM range for all the β-lactams assayed. By using cephalotin, Michaelis-Menten curves fit to a mixed hyperbolic inhibition model with a predominant uncompetitive component. A substrate inhibition occurred only when the V_HH is bound.

A.

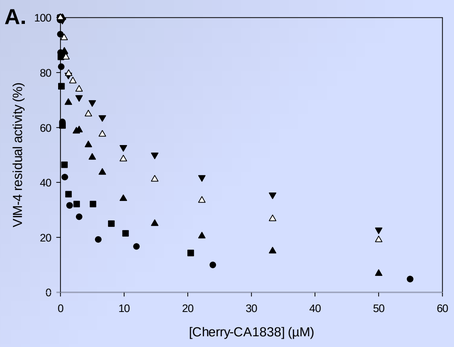

B.

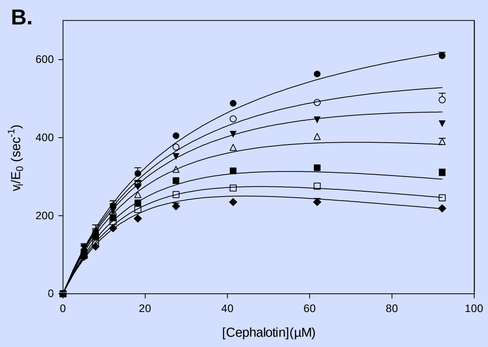

C.

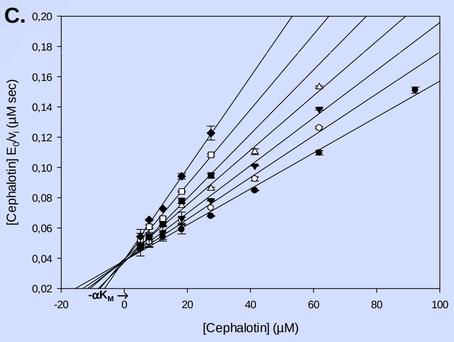

D.

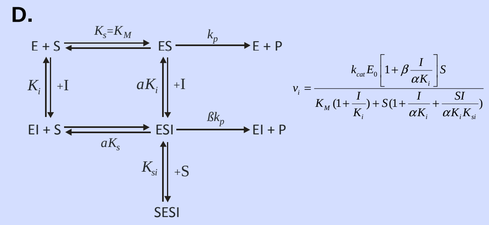

k_{cat} (s^{-1})	K_M (µM)	α	β	K_i (µM)	K_{si} (µM)
820 ± 17	31 ± 2	0.6 ± 0.2	0.4 ± 0.1	9 ± 2	45 ± 14

A. fractional activity plot using 25 µM imipenem (●); 175 µM benzylpenicillin (■) and 15 µM (▼); 50 µM (Δ) and 80 µM (▲) of cephalotin.
B. Global analysis of Michaelis-Menten curves using equation in D. [Cherry-CA1838]: (●) 0 µM; (○) 0.5 µM; (▼) 1 µM; (Δ) 2 µM; (■) 4 µM; (□) 6 µM; (♦) 8µM. R^2: 0.9954
C. Hanes-Woolf linearization of inhibitions curves. Data points high above apparent K_M are removed in order to see the converging lines beyond the y-axis typical of a predominantly uncompetitive mixed inhibition type. [Cherry-CA1838]: (●) 0 µM; (○) 0.5 µM; (▼) 1 µM; (Δ) 2 µM; (■) 4 µM; (□) 6 µM; (♦) 8µM.
D. Scheme representing the inhibition model and steady state parameters obtained by global fitting.

IV. Epitope mapping

Epitope mapping: scanning and truncation peptide arrays allowed us to define the conformational epitope of CA1838 as being composed of two amino-acids stretches that are in close proximity, solvent exposed and distant from the active site. (i.e. LPVTRA and VLRAAG)

A.

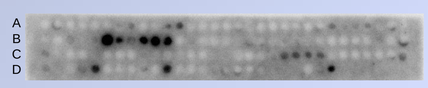

B.

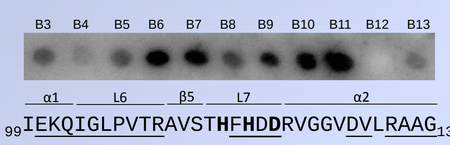

$_{99}$IEKQIGLPVTRAVSTHFHDDRVGGVDVLRAAG$_{133}$

C.

```
(B3)IEKQIGLPVTRA
(B4)  KQIGLPVTRAVS
(B5)    IGLPVTRAVSTH
(B6)      LPVTRAVSTHFH
(B7)        VTRAVSTHFHDD
(B8)          RAVSTHFHDDRV
(B9)            VSTHFHDDRVGG
(B10)             THFHDDRVGGVD
(B11)               FHDDRVGGVDVL
(B12)                 DDRVGGVDVLRA
(B13)                   RVGGVDVLRAAG

(D11:loop L12)        GH-GLPGGLDLLQ
```

D.

Positive (by dercreasing density)	Negative (No density at all)
EKQIGLPVTRAVSTHFHDDRVGGVDVLRAAG	
RAVSTHFHDDR_(A17)	IEKQIG_(C14)
VTRAVSTHFHD_(A16)	IEKQIGLP_(B18)
RAVSTHFHDDRV_(A6)	IEKQIGLPV_(B5)
RAVSTHFHD_(B10)	IEKQIGLPVT_(A24)
VLRAAG_(C27)	VSTHFHDDRVGG_(A7)
LPVTRAVS_(B21)	THFHDDRVGGVD_(A8)
IGLPVTRAV_(B7)	FHDDRVGGVDVL_(A9)
IGLPVTRAVS_(A26)	DDRVGGVDVLRA_(A10)
LPVTRA_(C17)	VSTHFHDDRVG_(A18)
IGLPVTRAVST_(A14)	THFHDDRVGGV_(A19)
IGLPVTRA_(B20)	FHDDRVGGVDV_(A20)
LPVTRAV_(C3)	DDRVGGVDVLR_(A21)
LPVTRAVST_(B8)	VGGVDVLRAAG_(A23)
LPVTRAVSTH_(A27)	VSTHFHDDRV_(A30)
IGLPVTR_(C2)	THFHDDRVGG_(A31)
RVGGVDVLR_(B15)	FHDDRVGGVD_(B1)
RVGGVDVLRA_(B3)	DDRVGGVDVL_(B2)
VTRAVS_(C18)	GGVDVLRAAG_(B4)
VTRAVST_(C4)	VSTHFHDDR_(B11)
KQIGLPV_(C1)	THFHDDRVG_(B12)
VTRAVSTH_(B22)	FHDDRVGGV_(B13)
RVGGVDVLRAA_(A22)	DDRVGGVDV_(B14)
IEKQIGLPVTR_(A12)	GGVDVLRAA_(B16)
IEKQIGLPVTRA_(A1)	GVDVLRAAG_(B17)
RVGGVDVLRAAG_(A11)	VSTHFHDD_(B24)
IGLPVTRAVSTH_(A3)	THFHDDRV_(B25)
VTRAVSTHFH_(A28)	FHDDRVGG_(B26)
RAVSTHF_(C5)	DDRVGGVD_(B27)
LPVTRAVSTHFH_(A4-B6)	RVGGVDVL_(B28)
RAVSTHFH_(B23)	GGVDVLRA_(B29)
VTRAVSTHF_(B9)	VDVLRAAG_(B30)
KQIGLP_(C15)	VSTHFHD_(C6)
KQIGLPVTRA_(A25)	THFHDDR_(C7)
KQIGLPVTR_(B6)	FHDDRVG_(C8)
	DDRVGGV_(C9)
	RVGGVDV_(C10)
	GGVDVLR_(C11)
	DVLRAAG_(C13)

THRESHOLD 20

A. Scanning peptide array of VIM-4 showing a conformational epitope for the V_HH CA1838.
B. Amino-acid sequence of the conformational epitope. (Spot B3-B13: I_{99}-G_{133})
Secondary structures are labelled. Zn^{2+} coordinating amino-acids are in bold and solvent exposed residues are underlined.
C. Overlapping peptides B3 to B13. Exposed amino-acids thought to be the main determinant for binding are highlighted by dark grey shading. Light grey shading represents amino-acids giving rise to artifactual signals that would be due to the array format, as suggested by similar peptide D11.
D. Truncation analysis of the epitope realized by peptide array. The left column in the table shows by decreasing density the truncated peptides still recognized by CA1838. No density was observed for peptides in the right column. Residues in yellow (loop L6 and C-terminal α2 helix) are determinant for binding whereas residues in red and magenta (active site loop L7 and N-terminal α2 helix) are not.

V. Epitope

Substituting the epitope by the the corresponding sequence of BlaB results in a chimeric functional MβL that is not recognized by the V_HH.

A.

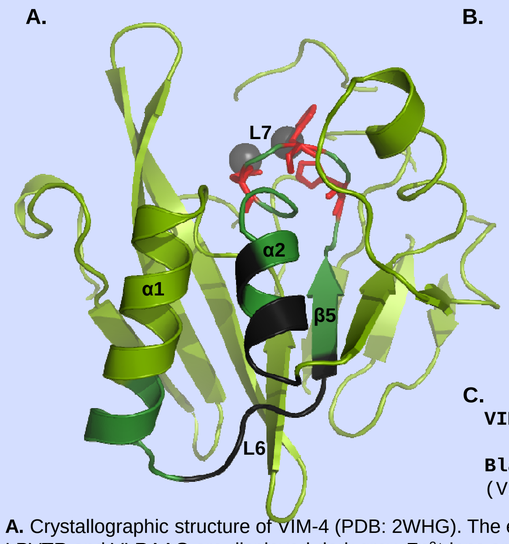

B.

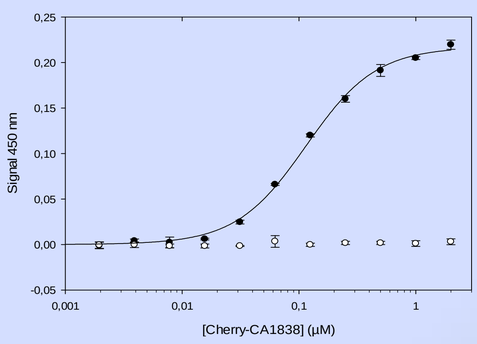

C.

```
                α1      L6      β5    L7        α2
VIM-4: LLAEIEKQIGLPVTRAVSTHFHDDRVGGVDVLRAAGVATY
                ** *: *  *    ::** ****.**:: :   *. **
BlaB:  FTDEIYKKHGKKVIMNIATHSHDDRAGGLEYFGKIGAKTY
(VIMΔepitope)
```

A. Crystallographic structure of VIM-4 (PDB: 2WHG). The epitope region I_{99}-G_{133} is in dark green. Amino-acids stretches LPVTR and VLRAAG are displayed dark grey. Zn^{2+} ions are in grey sphere, Zn^{2+} coordinating amino-acids of loop L7 are in red sticks.
B. ELISA experiment with coated WT VIM-4 (●) and coated VIMΔepitope (○). VIMΔepitope corresponds to VIM-4 MβL whose epitope has been substituted by the corresponding sequence of BlaB, which results in a chimeric functional MβL which is not recognized by the V_HH CA1838.
C. The main differences between the epitope corresponding sequences of VIM-4 and BlaB are found in loop L6 and in the C-terminal part of helix α2, which emphasized the importance of these two stretches for binding. (see alignment)

Because the V_HH CA1838 binds to a site distant from the active-site and alters both substrate binding and catalytic properties of VIM-4, this V_HH qualify to the definition of an allosteric effector with kinetic parameters α and β (table 1) quantifying the allosteric coupling.
MD studies have identified a local flip of the active site loop L7 that would be a conformational response to the increase in Zn-Zn distance upon binding of a ligand in the active-site (Salsbury *et al*, 2009). Binding of CA1838 could prevent such a dynamic flip, thereby acting as an allosteric inhibitor of VIMs MβLs.

This work was supported by FRIA (FNRS) and the Belgian Science Policy.